Lipids and Proteins Differentiation in Membrane Fouling Using Heavy Metal Staining and Electron Microscopy at Cryogenic Temperatures

Hélène Roberge, Philippe Moreau, Estelle Couallier, Patricia Abellan

Lipids and proteins differentiation in membrane fouling using heavy metal staining and electron microscopy at cryogenic temperatures

Hélène ROBERGE[1,2]*, Philippe MOREAU[1] , Estelle COUALLIER[2], Patricia ABELLAN[1]*

[1] Nantes Université, CNRS, Institut des Matériaux de Nantes Jean Rouxel, IMN, F-44000 Nantes, France

[2] Nantes Université, CNRS, ONIRIS, Laboratoire de Génie des Procédés, Environnement et Agroalimentaire, 7 GEPEA, F-44600 Saint-Nazaire

*Corresponding authors: helene_roberge@hotmail.fr ; Patricia.Abellan@cnrs-imn.fr

Keywords

Cryo-TEM; cryo-SEM; heavy metal staining; biomolecule differentiation in EM; membrane fouling

Abstract

The detailed characterization of fouling in membranes is essential to understand any observed improvement or reduction on filtration performance. Electron microscopy allows detailed structural characterization and its combination with labelling techniques using electron-dense probes typically allows for the differentiation of biomolecules. Developing specific protocols that allow for differentiation of biomolecules in membrane fouling in electron microscopy is a major challenge due to both: the necessity to preserve the native state of fouled membranes upon real filtration conditions as well as the inability of the electron-dense probes to penetrate the membranes once they have been fouled. In this study, we present the

development of a heavy metal staining technique for identification and differentiation of biomolecules in membrane fouling, which is compatible with cryofixation methods. A general contrast enhancement of biomolecules and fouling is achieved. Our observations indicate a strong interaction between biomolecules: a tendency of proteins, both in solution as well as in the fouling, to surround the lipids is observed.. Using TEM and cryo-SEM in combination with EDX, the spatial distribution of proteins and lipids within fouling is shown and the role of proteins in fouling discussed.

Introduction

Membrane filtration processes using porous polymer membranes allow concentrating, separating and purifying the components from a complex mixture in a liquid phase. Recently, they have been adapted for microalgae biorefining, where filtration, is used to separate and recover valuable metabolites from ground microalgae aqueous extracts (Lorente et al., 2017; Safi et al., 2017). The biomolecules recovered using membrane filtration can then be used in pharmaceutical industry, cosmetics, food supplements or biofuel industry as biodiesel (Clavijo Rivera et al., 2020; Villafaña-López et al., 2019). The biorefining is still a challenge that drives many research works over the last decade to fully exploit different fractions after the biomass harvesting. During filtration, unwanted accumulation of biomolecules on the surface and in the pores of the membrane, known as fouling, hinders membrane performance and is the main technical obstacle to improving the filtration of microalgae extracts for industrial applications (S. Liu et al., 2021).For example, after the cell disruption of protein rich microalgae and the production of a clarified aqueous extract, its microfiltration allows only a small recovery of proteins (up to 10-20%) in the permeate, which has led different research groups to suggest that they could be retained in macromolecular complexes or aggregates (S. Liu et al., 2021, 2022; Safi et al., 2017; Ursu et al., 2014). In order to directly probe the precise interaction of

biomolecules in fouled membranes and to design new processes aimed at an efficient recovery of valuable biomolecules from microalgae, a detailed characterization of fouling is needed. Despite a large volume of work devoted to characterize fouling, it has not been fully described or explained in the literature (Chen et al., 2018; Rudolph et al., 2019; Suwal et al., 2015; Tummons et al., 2020).

Microalgae produce proteins containing essential amino acids, polysaccharides with texturing or antibacterial properties, lipids such as triglycerides, antioxidant polyunsaturated fatty acids (DHA, EPA), pigments like carotenoids, terpenes. Fouling with microalgae extracts is therefore a very complex process where interactions between a large number of different biomolecules occur. In order to investigate membrane filtration processes and fouling formation, model mixtures of biomolecules are typically produced to separate the interactions of a small set of target compounds (Clavijo Rivera et al., 2020). Of particular relevance is the use of model solutions allowing the study of the impact of lipids and proteins within the microalgae extracts on membrane filtration since these are two of the most sought-after biomolecules from microalgae (Clavijo Rivera et al., 2020; Couallier, 2019; S. Liu et al., 2022). The performance of the membrane filtration process (productivity and selectivity) is impacted by the nature of the filtered solution itself. For example, the filtration of lipids alone presents a better flux than when proteins are added, leading to the assumption that the presence of proteins may decrease the filtration performance. Previous work has suggested that proteins could block the pores of the membrane (Couallier, 2019; Suwal et al., 2015) or involve a high retention of lipids on the membrane surface. However, these hypotheses could not be verified so far. Thus, a better understanding of the interactions between lipids and proteins, as well as their organization at the surface and in the porous medium, are necessary to understand membrane fouling. Strategies to limit fouling and improve process performance could then be proposed.

Generally, lipids and proteins can organize in a wide range of colloids with sizes from very small to relatively large (between 10 nm and 100 µm in diameter). The former one gather in stable spherical droplets (Clavijo Rivera et al., 2018; Gennes & Brochard-Wyart, 2015; S. Liu et al., 2022; Villafaña-López et al., 2019) while the later one appear as aggregates, filaments or soluble molecules in liquid phase (Linder, 2009; Stradner et al., 2004). When the two types of biomolecules are mixed, a strong reorganization occurs, due to interactions between them, generating a modification of the suspension to be filtered (size of droplets and aggregates for example) (Linder, 2009; Stradner et al., 2004). In particular, in the presence of lipids, proteins can organize themselves into intermediate layers at the interface between oil and water (Damodaran, 2005).

Electron microscopy techniques (EM) are now expanding to characterize ultrafiltration (UF) and microfiltration (MF) polymer membranes. Notably, FIB/SEM allows the characterization of the internal nanoporous structure of the material in 3D with a few cubic nanometer resolution (Brickey, et al., 2021; Roberge et al., 2022; Sundaramoorthi et al., 2016). In addition, the use of Energy-dispersive X-ray spectroscopy (EDX) and transmission electron microscopy (TEM) provides additional chemical and structural information with high spatial resolution (Kłosowski et al., 2016; Lin et al., 2016; Pacheco et al., 2010). One of the major challenges in the characterization of fouled membranes is the differentiation of biomolecules mixed within the fouling. Biomolecules are composed of light elements such as carbon, nitrogen, oxygen or hydrogen, and thus present low image contrast (Frank, 2006; J. Liu et al., 2019). Additionally, lipids and small proteins agglomerates can present similar size and shape. During electron microscopy observations, the use of staining agents is commonly used for localization and differentiation of biomolecules. Staining methods, thus, could be applied in the field of filtration processes, to allow us to understand the architecture of fouling, both on the surface (external fouling) and within the membrane (internal fouling).

When labelling fouled biomolecules in filtration membranes using electron dense probes, there are several major technical challenges to anticipate. One is the inability of staining agents (which are usually applied in solution) to penetrate through the external membrane fouling and through the fouled membrane pores. This is particularly true when relatively large volumes, as those probed by FIB/SEM (as opposed to thin films by TEM) are characterized. Labelling the different biomolecules prior to filtration could be a solution to this problem, which has not been explored before. Another technical challenge is keeping the fouled membrane as closely as possible to the real filtration conditions during observations. Conventional sample dehydration for EM was reported to destroy the fouling structure (Gusnard & Kirschner, 1977; Mollenhauer, 1993). The use of cryotechniques can be a solution to this issue and indeed, electron microscopy techniques at cryogenic conditions have been widely applied in biology (observation of cells, tissues or samples with a lot of artefacts due to dehydration) (Thompson et al., 2016), and are starting to be applied to material sciences (alternative for imaging sensitive materials, such as organic materials (Franken et al., 2017)). Despite their promise, however, they have not been applied yet for the characterization of filtration membranes fouled by biomolecules. Finally, if cryotechniques are used to preserve the hydrated state of fouled membranes, staining methods that are compatible with cryogenic sample preparation must be applied.

One of the most successful methods for macromolecular detection in electron microscopy is immunolabeling. Immunostaining requires extensive expertise and has traditionally been used for functional imaging (Beesley, 1989; Carrassi et al., 1990; Sarraf, 2000), i.e. it is suitable for specifically localizing molecules in a medium, such as a cell (Marion & Trichet, 2018; Ripper et al., 2008). It is most commonly done prior to dehydration of the sample (either before or after resin embedding), which is not compatible with observing fouling on hydrated membranes. It also requires the use of soft fixatives to preserve epitopes, which damages the ultrastructure, in addition to the effects of dehydration and resin inclusion (Beesley, 1989; Giepmans, 2008). For

the case of cryofixated samples, several preparation techniques are possible which have only been applied to thin films for TEM analysis. They can be separated into two categories: immunolabeling of (i) an internal object and (ii) an external object (within a matrix or a cell). In the case of biomolecules determination within fouled membranes, these two categories would correspond to the labelling of the biomolecules after filtration and fouling, case (i), or labelling of the biomolecules prior to filtration and fouling, case (ii). Immunolabeling of an internal object has the disadvantage of damaging the ultrastructure due to the use of detergents to allow internal penetration of antibodies, as well as a saturator of sites (often BSA, bovine serum albumin) to avoid false positives (Beesley, 1989; Marion & Trichet, 2018) and thus, it could modify both the fouling and the structure of filtration membranes. Regarding immunolabeling of an external object, although this option could allow for easy penetration of the labelled biomolecules through the membrane and would also be compatible with cryofixation of the membranes after filtration, it requires additional chemical modification of the membranes prior to filtration to allow the bonding (Giepmans, 2008), which will interfere with the natural filtration process.

Another solution for achieving macromolecular imaging in electron microscopy is to enhance image contrast with the addition of heavy metals (M. A. Hayat, 2000). Indeed, biological materials, containing lipids and proteins such as those in this study, possess specific sites or structures that facilitate chemical bonding with heavy metals (Gloaguen, 2010; J. Liu et al., 2019; Rames et al., 2014). For example, Sato et al (Sato et al., 2019), used uranyl acetate or osmium tetroxide, for identification of proteins, nucleic acids, and lipids within an animal tissue and Monneron and Bernhard(Monneron & Bernhard, 1969) used it to differentiate RNA from DNA. This is not typically the case for polymers, which do not have such sites. General contrast enhancement, however, is possible in polymeric membranes by absorption of heavy metals (Gloaguen, 2010; Trent, 1984). Importantly, heavy metal staining can be performed on

the biomolecules prior to filtration thus allowing for the use of cryofixation techniques without the need of chemical modification of the membranes.. Furthermore, heavy metal staining protocols are more cost-effective than immunolabeling, easier to adopt, faster, and generates less bias(Hayat, 1975).

In this study, the development of a heavy metal staining technique is presented for the identification and differentiation of the biomolecules (lipids and proteins) which constitute membrane fouling. A general contrast enhancement of the biomolecules and the fouling, compared to the polymeric filtration membrane, has been accomplished. Both types of stained biomolecules are observed alone and then mixed on the surface of a fouled MF PES membrane. Thanks to this development, the staining allows the differentiation of lipids and proteins not only within a model mixture, but also within the fouling of a membrane by both TEM and cryo-SEM of cross-sectional FIB sections.

2. Materials and Methods

2.1 Materials

2.1.1 Conditioning of biomolecule solutions

The use of model mixtures, more stable and with a composition and properties (conductivity, pH, concentration…) similar to real mixtures, allows us to reproduce the behavior of microalgae extracts during membrane filtration (Clavijo Rivera et al., 2020; Villafaña-López et al., 2019). In this study, lipid (S_L), protein (S_P) and mixed lipids and proteins ($S_{LP)}$ solutions were used. The solutions were prepared following protocols published elsewhere (S. Liu, 2021) and stabilized by a phosphate buffer (pH 7.4, Conductivity 790 µS·cm-1, close to Parachlorella kessleri culture medium properties).

2.1.2 Membrane conditioning

A flat-sheet commercial microfiltration membrane of polyethersulfone (PES), with an average nominal pore diameter of 0.1 μm (Koch membrane systems, USA), was analyzed. Prior to its characterization, the membrane was conditioned following the procedure reported by Rouquié et al (Rouquié et al., 2020, 2022) and described in Roberge et al (Roberge et al., 2022).

2.1.3 Membrane fouling and storage

The stained solutions (S_L, S_P or S_{LP}) were individually filtered using an Amicon® cell with a transmembrane pressure of ≈ 0.45 bar and stirring of 300 rpm, (S. Liu, 2021) as previously performed.

The solutions were filtered through the PES membrane until the flow decreased and stabilized (between 3 and 6 h of duration), showing the presence of a stable fouling. After the filtration, the membrane was rinsed with water and stored in a box at 4°C with a little water to keep the sample hydrated. EM observations were carried out as soon as possible after filtration to analyze the freshest fouled membrane (risk of contamination by microorganisms or drying of the membrane and its fouling over time).

2.1.4 Final staining protocols using Uranyless® and PTA

The S_L and S_P solutions were individually stained with 1% of Uranyless® and PTA (Phosphotungstic acid, in solution, HT152-250ML, Sigma-Aldrich) respectively and mixed to obtain the S_{LP} considering the respective concentrations of the biomolecule solutions. Note that the concentration of staining (1%) was chosen based on similar contrast protocols (Hayat, 1975).

The stained solutions were left under agitation for 20 minutes. Then, the S_L was left without stirring for 15 minutes. In this way, the excess Uranyless® has been removed from the surface of the final lipid solution. The S_P was centrifuged for 5 minutes at 5000 g and the PTA phase was removed (bottom). This technique allows limiting false positives (identification of markers without presence of biomolecules during EM analysis). After staining, the solutions were homogenized again by shaking.

2.2 Methods

2.2.1 Characterization by TEM, STEM and EDX

Prior to their use, the TEM grids (Carbon Film, 400 mesh) were hydrophilized (to allow easier deposition of a solution of minimal thickness) using a plasma cleaner (Fischione Instruments, model 1070) with pure argon gas for 5 minutes and with a 30 % power and a gas flow of 30 sccm. The hydrophilic property of the grids is maintained between 30 minutes and 1 hour. A droplet of sample solution is placed on a grid for 5 minutes. The excess is then removed by contact with a Whatman® paper and the grid is stored in a sample dish (allowing it to dry). The grids are prepared in duplicate and at least 4 h before their observation in TEM in order to minimize the water content.

TEM images were acquired using a Hitachi H-9000 NAR TEM operated at 300 kV to test the effect of the different contrast enhancement protocols in TEM images. STEM images and EDX analyses were performed using a S/TEM Themis Z G3 (Thermo Fisher Scientific), operated at 300 kV and equipped with the ChemiSTEM™ Super-X EDX detector, consisting of four silicon drift EDX detectors (SDD). STEM imaging was performed using a HAADF detector and beam current of 65 pA. EDX maps of 512x512 pixels and 1024x1024 pixels were acquired with a pixel size of 5 to 10 nm. Between 70 and 250 frames with a dwell time of 10 µs

were acquired to limit instantaneous beam damage but allow for enough statistics. The software Velox® (3.5.0.952 version) was used to process the data.

2.2.2 Cryofixation of fouled membranes and Cryo-SEM characterization

A dual FIB/SEM Zeiss Crossbeam 550L, equipped with a Quorum® PP3010 Cryo-FIB/SEM preparation system was used allowing for sample preparation (cryofixation) and transfer and observations at cryogenic temperatures. The PES membrane fouled with stained biomolecules was cryofixed by fast freezing into slush nitrogen. Then, the membrane was cryo-fractured with a blade in the SEM prep chamber and metalized with a thin layer of few nanometres of platinum to obtain a conductive coating. Finally, it was transferred under cryogenic conditions using the Quorum transfer system to the SEM chamber for observation.

SEM images were obtained with a SESI detector (10 keV, 1000 pA) and a pixel size between 10 and 100 nm. EDX was performed at cryogenic conditions in the Zeiss Crossbeam 550L microscope using an Oxford energy-dispersive spectrometer. The spectrometer is composed of an ULTIM® Max with a large silicon drift detector area (sensor area of 100 mm^2) and positioned at a take-off angle of ~35° from the sample. For EDX analysis, an incident beam energy of 7 or 15 keV, a current of about 1 nA and a dwell time of 100 µs were used. It should be noted that the energy was chosen according to the element to be detected, the rule being that the energy of the incident beam must be at least 2.7 times higher than the energy of the targeted emission line (Ruste, 1987). Here, 15 keV was chosen for the analysis of S_L and S_{LP} solutions, which contain lanthanum (La, found in Uranyless®, emission line L_α at 4.6 keV), and 7 keV for the analysis of SP, which contains tungsten (W, found in PTA, emission line M_α at 1.7 keV). No damage from the electron beam could be observed after the analysis.

3. Results

3.1 Identification and selection of the staining agents

In this study, OsO_4, RuO_4, Uranyless® as well as PTA were tested in order to contrast biomolecules, individually and then mixed, for EM. These products were selected based on the following criteria: A) they should present the highest possible specific affinity for both, or at least for one of the molecules and B) they should not be CMR (carcinogenic, mutagenic and toxic for reproduction), which also avoids the contamination of the filtration modules. Furthermore, C) the staining should be effective, not only to improve the imaging contrast, but also to allow its detection by the available EDX detectors.

Table 1: Comparison of the different staining agents selected and tested in this work, showing their ability (✓) or inability (X) to stain specific biomolecules or polymers, according to the literature (indicated by a citation) and to the experiments performed during this work (indicated by: "[this work]"). The CMR nature of the product as well as the possibility of detection by EDX using the Super X detector in the Nant'Themis were also indicated.

		Staining agent			
		Uranyless® (with La)	Osmium tetroxide (OsO_4)	Ruthenium tetroxide (RuO_4)	phosphotungstic acid (PTA) (with W)
Membrane	PES	X(Gloaguen, 2010)	✓ (Trent et al., 1983)	✓ (Trent et al., 1983)	X (Gloaguen, 2010)
	PAN	X (Gloaguen, 2010)	X (Trent et al., 1983)	X (Trent et al., 1983)	✓(Chen et al., 2005)
Biomolecules	Lipid	✓ (J. Liu et al., 2019) ; [this work]	✓(Hayat, 1975) ; X [this work]	✓ (Hayat, 1975) ; X [this work]	X(J. Liu et al., 2019; Sato et al., 2019)
	Protein	✓ (Sato et al., 2019; Trent et	X(Hayat, 1975)	X (Hayat, 1975)	✓ (Hayat, 1975; Rames et al., 2014) ; [this work]

		al., 1983) ; [this work]			
	CMR[a]	No	Yes	Yes	No
	EDX (TEM)	Yes (La, Gd)	Yes (Os)	Yes (Ru)	Yes (W)

a: Carcinogenic, Mutagenic or Toxic to Reproduction.

In Table 1 are presented the different candidates considered to contrast the biomolecules. The results from the literature and this work (presented below) are summarized. The different contrasting agents were compared according to their ability to contrast lipids, proteins, but also PAN and PES polymers, which are the constituents of filtration membranes. The staining should be as specific as possible.

Table 2: Comparison of the different staining agents selected and tested in this work, showing their ability (✓) or inability (X) to stain specific biomolecules or polymers, according to the literature (indicated by a citation) and to the experiments performed during this work (indicated by: "[this work]"). The CMR nature of the product as well as the possibility of detection by EDX using the Super X detector in the Nant'Themis were also indicated.

Although Osmium (OsO_4) and Ruthenium Tetroxide (RuO_4) were considered for staining of lipids following literature results (Hayat et al, 1975), our tests using these compounds showed degradation of the biomolecules upon staining (not shown). Moreover, their CMR character complicates experiments, by making necessary the establishment of specific treatments of wastes and cleaning procedures of the filtration modules and tools used. Thus, OsO_4 and RuO_4 were ruled out as appropriate candidates. We included them in table 1, with respect to observed discrepancy with the results from the literature.

Regarding the Uranyless®, it is commonly used in EM to stain biological samples and therefore it is compatible with the biomolecules used in this study (lipids and proteins). This compatibility was successfully verified for both types of biomolecules. However, although it enhances the overall contrast of biomolecules, a second staining agent is required to differentiate lipids from proteins. Finally, Phosphotungstic acid (PTA) is described in the literature to specifically target proteins and not lipids. After verification of this property, PTA was chosen to stain proteins and Uranyless® to stain lipids (highlighted in gray in Table 1). It should be noted that both staining agents are easy to use, cheap, detectable by EDX spectroscopy and not CMR.

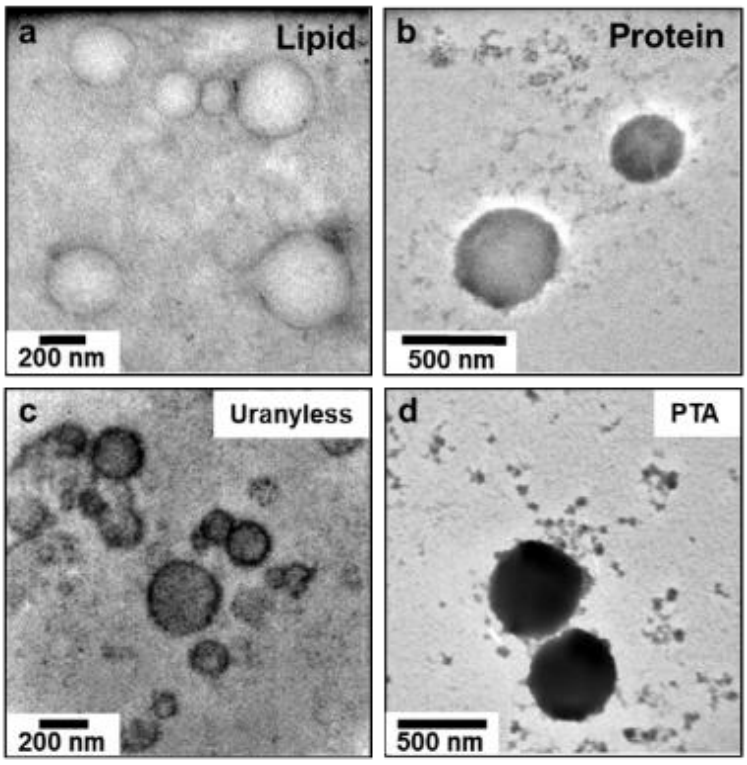

Figure 1 : TEM images of solutions after drop-casting and drying of 5 µL of SL solution (lipids, images on the left hand side) and 5 µL of SP solution (proteins, images on the right hand side) on a TEM grid. (a): Lipid aggregates, forming relatively large droplets without staining. (b): Protein aggregates without staining. (c): Lipid droplets observed after staining of the SL solution using Uranyless®. Contrast enhancement of the external bilayer membranes is observed. (d): Protein aggregates observed after PTA staining of the SP solution, displaying homogeneous contrast.

Considering the selective properties of PTA (see Table 1), its direct use on a S_{LP} containing the ready-mixed biomolecules was tested to label only the proteins (results not shown).

Unfortunately, the aggregates are already formed by lipid-protein interactions, and the PTA, which targets proteins, binds around the aggregate, and thus does not differentiate the biomolecules within. However, it allows a general contrast enhancement of the biomolecules.

Figure 1 shows TEM images of lipids (left) and proteins (right) before and after their staining with Uranyless® and PTA respectively. In Figure 1c, lipids show a higher contrast than in Figure 1a, with higher presence of Uranyless® on the surface of the lipids, depicting a ring-like contrast, consistent with the limitation of staining penetration into the lipid droplet. Similarly, Figure 1d shows proteins more contrasted than in Figure 1b, where in this case, PTA produces a homogeneous contrast enhancement, which is consistent with a homogeneous distribution of proteins and staining within the agglomerates in Figure 1.

3.2 Identification of mixed lipids and proteins by HAADF STEM and EDX

Figure 2 (i) and (ii) shows two regions of the same sample, a mixture of lipids and proteins previously stained with Uranyless® containing lanthanum (La) and PTA containing Tungsten (W), respectively. Regions indicated as a and b in the STEM image in Fig. 2 (ii) have been digitally enlarged to point out specific details in the images. The images were obtained using a HAADF detector and thus, contrast can be linked to chemistry variations (Z contrast) in the sample and to thickness. Images show mostly rounded particles, many of which present brighter contours with a size between a few nanometers and a few hundred nanometers of diameter, consistent with the presence of lipids. Other objects display either spherical morphology with homogeneous contrast or a filament-shaped morphology, and have a size from a few nanometers to a few micrometers in diameter or length. These homogeneous spheres and filaments appear in many cases to be positioned around the ring-like features (lipids) and may be associated with protein agglomerates. Although differences in size, contrast homogeneity

and morphology are thus observed, and considering the strong interactions between biomolecules in complex mixtures reported in the literature (J. Liu et al., 2019), additional data is required in order to separate and identify the different biomolecules. EDX analysis was performed to this end.

Figure 2 (bottom) shows an overlay of EDX maps obtained for the areas imaged (STEM images in Figure 2 top) using the lanthanum (La), in red, and tungsten (W), in green. These elements are present in Uranyless® (used for lipid staining) and PTA (protein staining) (see Table 1), respectively, and thus reveal the position of lipids (in red) and proteins (in green) in the image.

From the EDX analysis, it is observed that a large part of the solution consists of an intimate mixture of proteins and lipids. It should be noted that some regions appear as yellow color, indicating the presence of lipids and proteins in the same area. These results are consistent with previous observations and demonstrate the complex interaction between lipids and proteins. Areas containing spheres with the stained contour are labeled in red (La), in consistency with the presence of lipids (visible in Figure 2(i) and the enlarged area b). Large green areas (without apparent lipids intermixing) are observed, such as the globule in the lower right-hand side of the image (ii) or the enlarged image b, and are consistent with the presence of larger protein agglomerates. Notably, green areas (W), consistent with a large presence of proteins, are mostly observed on and around the lipids. This observation indicates that the proteins in the solution, even when they do not agglomerate, will tend to surround the lipids, which will have strong consequences in fouling.

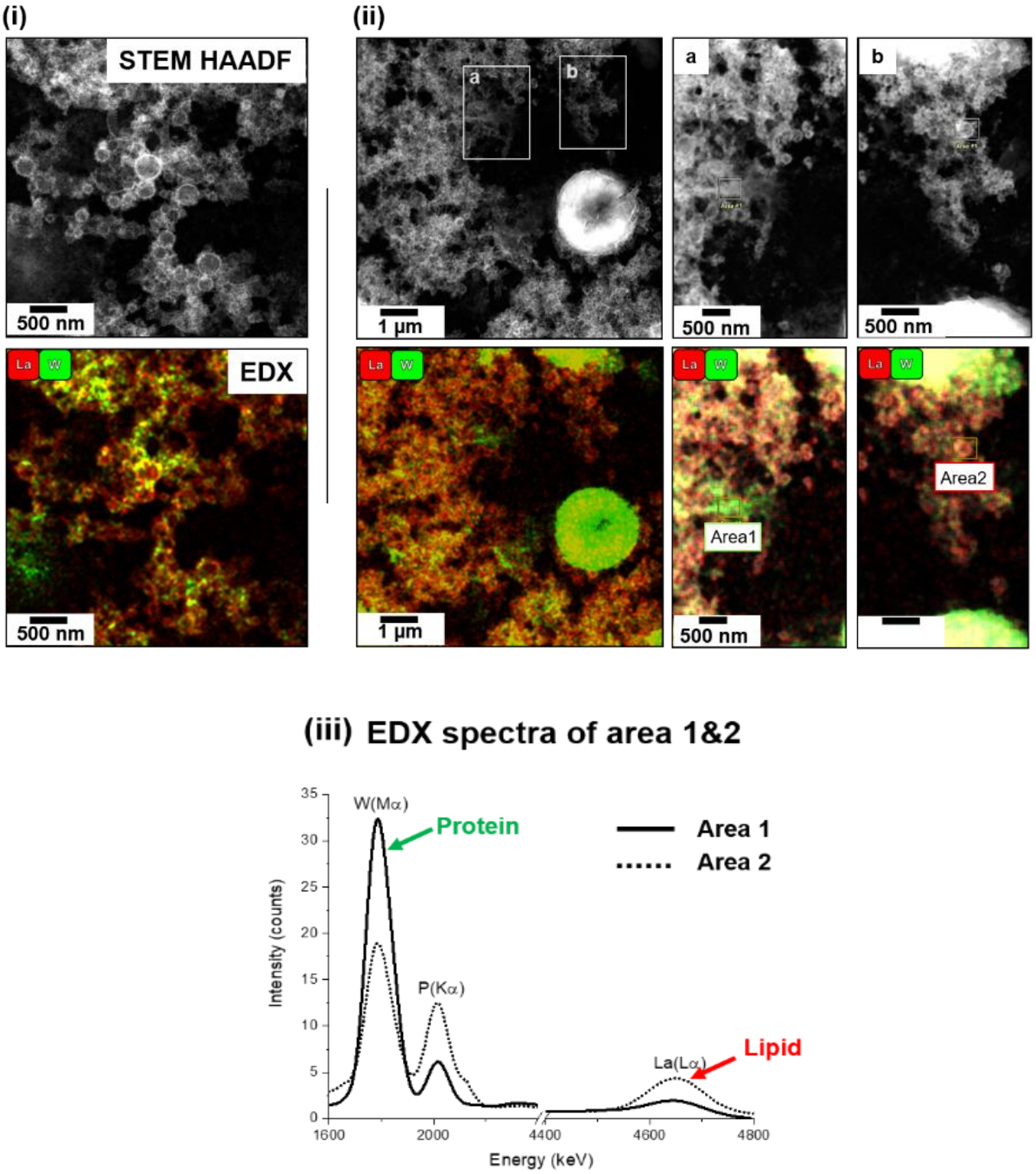

Figure 1: HAADF STEM image (i) and EDX analysis (ii and iii) of a stained lipid and protein mixture solution with Uranyless® (La in red) and PTA (W in green), respectively.

Figure 2 (iii) shows EDX spectra averaged over Area 1 (a protein-rich area as indicated in the EDX maps) and Area 2 (consistent with a lipid droplet, based on image contrast and the red color in the EDX map). In area 1, a W peak (Mα energy line) with a high intensity is observed

and the presence of a La peak (Lα energy line) with a lower intensity is noted. While in area 2, a W peak (Mα energy line) is also observed, but with a lower intensity than in area 1 as well as a La peak (Lα energy line) with a higher intensity. The presence of the W peak in the lipid area is an indicator of the existence of proteins in the same region, and confirms the strong interactions between biomolecules. Since the biomolecule markers have now been identified, it is necessary to verify if this observation is also possible within the membrane fouling. This will be probed below.

3.3 Identification of lipids and proteins on a fouled membrane by SEM and EDX under cryogenic conditions

In order to test the methods described above for the differentiation of lipids and proteins on fouled membranes, a PES membrane fouled with a model mixture of stained biomolecules in the Amicon® cell was characterized by SEM/EDX. In order to observe the fouling as close as possible to native conditions, cryofixation of the sample was performed and observations were performed at cryogenic temperatures. Figure 3 shows cross-sectional images of the fouled PES filtration membrane. The images were obtained by cryo-SEM (SE) imaging, under cryogenic conditions (upper part of the figure) and by cryo-EDX analysis (lower part of the figure). The red rectangles indicate the enlarged areas on the right-hand side of the figure. For the cryo-SEM images, the fouled membrane was fractured, after freezing, using a pivot-mounted knife in the SEM cryo prep-chamber, to observe the interior of the porous medium. In this way, the different layers of the membrane are visible. In particular, a few micrometers thick layer of biomolecules is observed at the surface of the membrane. This is an external fouling that can be described as a "cake" of biomolecules (Yu et al., 2021). Consistently with previous observations, it is difficult to differentiate lipids and proteins in this fouling layer, using only cryo-SEM (SESI)

images. We note that this was also the case for images acquired using both the InLens and BSE detectors (not shown).

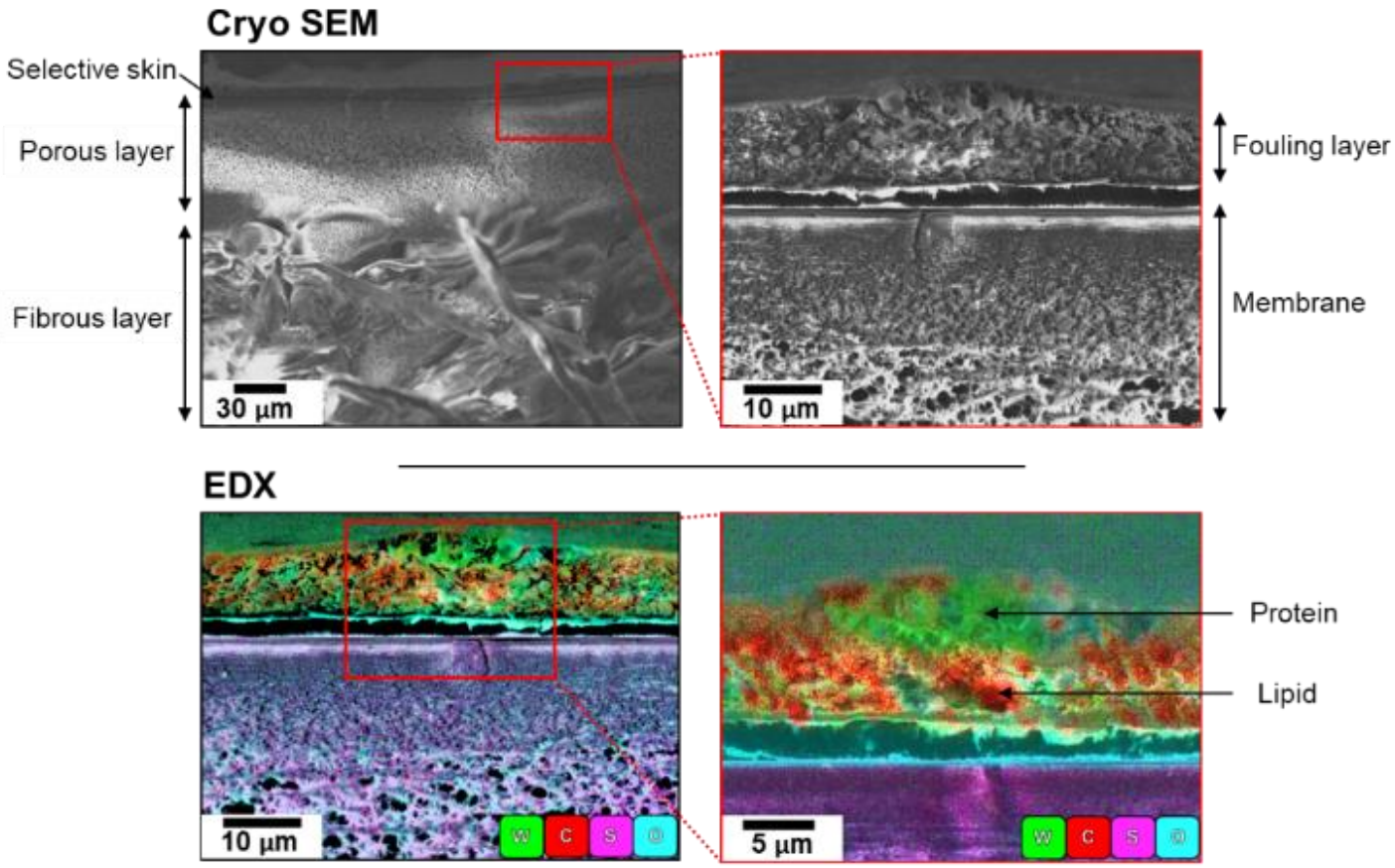

Figure 3: Cryo-SEM image and EDX analysis of cross section of a PES membrane fouled with stained biomolecules.

Note: C is in red in this image (versus La in red in Figure 2).

The lower part of Figure 3 shows a superposition of EDX maps with tungsten (W) in green, carbon (C) in red, sulfur (S) in pink and oxygen (O) in blue. It should be noted that the homogeneous presence of oxygen in the image is due to the cryogenic conditions (presence of water and thus ice inside the membrane and everywhere in the sample) and the composition of the sample (oxygen present in membrane and biomolecules). Concerning sulfur, it is one of the elements that compose the PES membrane and it is only minimally present in the biomolecules. Therefore, the delimitation of the membrane in space is possible due to the sulfur signal. The analysis reveals the position of the proteins (in green, W). Lanthanum (La), the lipid marker, was however not detected. This seems to be due to its concentration being too low, (below the

sensitivity of the EDX detector used in the SEM) and/or to the orientation of the sample in the SEM chamber with respect to the detector.

In order to verify this hypothesis, the sensitivity of the detector was evaluated by analysing, with the SEM, the TEM grid presented in Figure 2. In opposition to tungsten (W), lanthanum (La) was not detected by the SEM EDX detector on this grid in opposition to the previous TEM analyses. Therefore, although Uranyless® is relevant for the differentiation of biomolecules in TEM, in our case, the SEM analysis configuration does not allow it.

Nevertheless, lipids are mostly composed of C and can be mapped without staining using the C signal (in red) on the EDX cartography. Indeed, Figure 3 reveals the presence of a carbon signal, complementary to the one of proteins, in the fouling cake formed on the membrane surface.

A surface fouling can thus be observed, containing proteins and lipids that can be seen in the whole thickness of the fouling. A space, appearing to be water, is observed between the cake and the membrane, which could be due to a detachment of the cake from the membrane surface during the freezing experiments. The use of other cryofixation methods, such as high pressure freezing could minimize this effect. The proteins seem to be present at different locations: at the bottom of the fouling forming a layer, around lipid droplets, but also in concentrated areas that could be protein aggregates. This observation highlights the role of proteins in the membrane fouling: their adhesion to the membrane may initiate the fouling, then their interaction with lipids may induce the entrapment of the droplets and form a complex cake where both molecules are intimately combined. This observation will drive the future development of the separation process as it becomes clear from these detailed data that the separation of the biomolecules by filtration will only be possible by mitigating the interaction that has been demonstrated here. The staining method developed, in combination with cryofixation and electron microscopy opens up the previously barely accessible black box of

the membrane fouling processes. It is of major interest for the understanding of the fouling, which is the main bottleneck in membrane processes, in many applications.

Conclusion

A heavy metal staining technique in (cryo) electron microscopy of lipids and proteins with Uranyless® and PTA, respectively, has been developed. This technique, essential to overcome the low contrast of biomolecules, allows to differentiate them within the fouling of filtration membranes. The heavy metal staining technique developed in this study allowed us to enhance the general contrast of biomolecules and to differentiate object aggregates, supposedly lipids and proteins, according to their morphologies, contrast and size in STEM. Then, by EDX mapping, the distribution of heavy metals is observed and consequently a differentiation between lipids and proteins is demonstrated possible. Finally, the analysis of a precise area with the acquisition of an EDX spectrum allows, in case of any doubt, to confirm the presence of specific markers of the observed biomolecules. In addition, lipids and proteins accumulated on the surface of a filtration membrane, were differentiated using cryo-SEM and EDX spectroscopy. In the latter case, we propose to use the C signal for SEM whenever the Lanthanum signal falls below the detection limit of the EDX detector.

In agreement with the previous observations, the proteins seem to present a important role in the membrane fouling. Notably, their adhesion to the membrane may initiate the fouling and their strong interaction with lipids may induce the formation of aggregates and a complex cake containing both molecules. These observations will lead to a better understanding of fouling, which is the main bottleneck in membrane filtration, and then develop fouling-limiting processes.

To go further and know, e.g., the spatial distribution of the different types of biomolecules in the fouling, a 3D acquisition by FIB/SEM coupled with EDX spectroscopy and cryogenic

conditions would allow to obtain more information. This technique could be explored in the future. Finally, this technique could be applicable in other fields (e.g. in biology with differentiation of lipid and protein in a cell (Sato et al., 2019) or in protein structure analysis (Rames et al., 2014)), allowing staining, identification and differentiation of objects within samples, not only for TEM imaging but also for SEM imaging, with cryogenic conditions or not.

Acknowledgements

HR thanks Nicolas Stephant for his valuable help on the ZEISS crossbeam microscope and Dr Eric Gautron & Nicolas Gautier for their valuable help on the EDX acquisitions and analysis on the (S)TEM microscope Nant'Themis. The authors would like to thank the financial support provided by the NExT initiative through the French National Research Agency (ANR) under the Programme d'Investissements d'Avenir (with reference ANR-16-IDEX-0007). The e-BRIDGE project also received financial support from the Pays de la Loire region and Nantes Métropole. FIB/SEM reconstructed volumes were collected in the CIMEN Electron Microscopy Center in Nantes funded by the French Contrat Plan État-Région and the European Regional Development Fund of Pays de la Loire.

Competing interests: The author(s) declare none

Bibliography

Beesley, J. E. (1989). Immunolabelling and electron microscopy in cytochemistry. *Current Opinion in Immunology*, *2*(6), 927-931. https://doi.org/10.1016/0952-7915(89)90180-5

Brickey, K. P., Zydney, A. L., & Gomez, E. D. (2021). FIB-SEM tomography reveals the nanoscale 3D morphology of virus removal filters. *Journal of Membrane Science*, 119766. https://doi.org/10.1016/j.memsci.2021.119766

Carrassi, A., Zambon, J. J., & Vogel, G. (1990). A new method of bacterial identification using gold immunolabelling and scanning electron microscopy. *Archives of Oral Biology*, *35*, S177-S180. https://doi.org/10.1016/0003-9969(90)90152-Z

Chen, W., Qian, C., Zhou, K.-G., & Yu, H.-Q. (2018). Molecular Spectroscopic Characterization of Membrane Fouling : A Critical Review. *Chem*, *4*(7), 1492-1509. https://doi.org/10.1016/j.chempr.2018.03.011

Chen, W., Zhu, M., Song, S., Sun, B., Chen, Y., & Adler, H.-J. P. (2005). Morphological Characterization of PMMA/PAN Composite Particles in Nano to Submicro Size. *Macromolecular Materials and Engineering*, *290*(7), Article 7. https://doi.org/10.1002/mame.200400291

Clavijo Rivera, E., Montalescot, V., Viau, M., Drouin, D., Bourseau, P., Frappart, M., Monteux, C., & Couallier, E. (2018). Mechanical cell disruption of Parachlorella kessleri microalgae : Impact on lipid fraction composition. *Bioresource Technology*, *256*, 77-85. https://doi.org/10.1016/j.biortech.2018.01.148

Clavijo Rivera, E., Villafaña-López, L., Liu, S., Vinoth Kumar, R., Viau, M., Bourseau, P., Monteux, C., Frappart, M., & Couallier, E. (2020). Cross-flow filtration for the recovery of lipids from microalgae aqueous extracts : Membrane selection and

performances. *Process Biochemistry*, *89*, 199-207. https://doi.org/10.1016/j.procbio.2019.10.016

Couallier, E. (2019). *Filtration membranaire de composés organiques en phase aqueuse* [Thesis, Université de Nantes, Faculté des sciences et des techniques]. https://hal.science/tel-02345764

Damodaran, S. (2005). Protein Stabilization of Emulsions and Foams. *Journal of Food Science*, *70*(3), Article 3. https://doi.org/10.1111/j.1365-2621.2005.tb07150.x

Frank, J. (2006). *Three-Dimensional Electron Microscopy of Macromolecular Assemblies : Visualization of Biological Molecules in Their Native State*. Oxford University Press.

Franken, L. E., Boekema, E. J., & Stuart, M. C. A. (2017). Transmission Electron Microscopy as a Tool for the Characterization of Soft Materials : Application and Interpretation. *Advanced Science*, *4*(5), 1600476. https://doi.org/10.1002/advs.201600476

Gennes, P.-G. de, & Brochard-Wyart, F. (2015). *Gouttes, bulles, perles et ondes*. Humensis.

Giepmans, B. N. G. (2008). Bridging fluorescence microscopy and electron microscopy. *Histochemistry and Cell Biology*, *130*(2), 211. https://doi.org/10.1007/s00418-008-0460-5

Gloaguen, J.-M. (2010). *Interest of staining techniques for M.E. observations of polymeric materials.*

Gusnard, D., & Kirschner, R. H. (1977). Cell and organelle shrinkage during preparation for scanning electron microscopy : Effects of fixation, dehydration and critical point drying. *Journal of Microscopy*, *110*(1), 51-57. https://doi.org/10.1111/j.1365-2818.1977.tb00012.x

Hayat, M. A. (1975). *Positive Staining for Electron Microscopy*. Van Nostrand Reinhold Company.

Kłosowski, M. M., McGilvery, C. M., Li, Y., Abellan, P., Ramasse, Q., Cabral, J. T., Livingston, A. G., & Porter, A. E. (2016). Micro-to nano-scale characterisation of polyamide structures of the SW30HR RO membrane using advanced electron microscopy and stain tracers. *Journal of Membrane Science*, *520*, 465-476. https://doi.org/10.1016/j.memsci.2016.07.063

Lin, L., Lopez, R., Ramon, G. Z., & Coronell, O. (2016). Investigating the void structure of the polyamide active layers of thin-film composite membranes. *Journal of Membrane Science*, *497*, 365-376. https://doi.org/10.1016/j.memsci.2015.09.020

Linder, M. B. (2009). Hydrophobins : Proteins that self assemble at interfaces. *Current Opinion in Colloid & Interface Science*, *5*(14), 356-363. https://doi.org/10.1016/j.cocis.2009.04.001

Liu, J., Wu, H., Huang, C., Lei, D., Zhang, M., Xie, W., Li, J., & Ren, G. (2019). Optimized Negative-Staining Protocol for Lipid-Protein Interactions Investigated by Electron Microscopy. *Methods in Molecular Biology (Clifton, N.J.)*, *2003*, 163-173. https://doi.org/10.1007/978-1-4939-9512-7_8

Liu, S. (2021). *Fractionnement de biomolécules issues de microalgues par filtration membranaire : Impact du milieu complexe sur les performances du procédé* [These de doctorat, Nantes]. http://www.theses.fr/2021NANT4016

Liu, S., Gifuni, I., Mear, H., Frappart, M., & Couallier, E. (2021). Recovery of soluble proteins from Chlorella vulgaris by bead-milling and microfiltration : Impact of the concentration and the physicochemical conditions during the cell disruption on the whole process. *Process Biochemistry*, *108*, 34-47. https://doi.org/10.1016/j.procbio.2021.05.021

Liu, S., Rouquié, C., Lavenant, L., Frappart, M., & Couallier, E. (2022). Coupling bead-milling and microfiltration for the recovery of lipids and proteins from Parachlorella

kessleri : Impact of the cell disruption conditions on the separation performances. *Separation and Purification Technology*, *287*, 120570. https://doi.org/10.1016/j.seppur.2022.120570

Lorente, E., Hapońska, M., Clavero, E., Torras, C., & Salvadó, J. (2017). Microalgae fractionation using steam explosion, dynamic and tangential cross-flow membrane filtration. *Bioresource Technology*, *237*, 3-10. https://doi.org/10.1016/j.biortech.2017.03.129

M. A. Hayat. (2000). *Principles and Techniques of Electron Microscopy | Biological imaging*. https://www.cambridge.org/gb/academic/subjects/life-sciences/biological-imaging/principles-and-techniques-electron-microscopy-biological-applications-4th-edition, https://www.cambridge.org/gb/academic/subjects/life-sciences/biological-imaging

Marion, J., & Trichet, M. (2018). *L'identification de molécules et structures en Microscopie Electronique en Transmission*. 26.

Mollenhauer, H. H. (1993). Artifacts caused by dehydration and epoxy embedding in transmission electron microscopy. *Microscopy Research and Technique*, *26*(6), 496-512. https://doi.org/10.1002/jemt.1070260604

Monneron, A., & Bernhard, W. (1969). Fine structural organization of the interphase nucleus in some mammalian cells. *Journal of Ultrastructure Research*, *27*(3), 266-288. https://doi.org/10.1016/S0022-5320(69)80017-1

Pacheco, F. A., Pinnau, I., Reinhard, M., & Leckie, J. O. (2010). Characterization of isolated polyamide thin films of RO and NF membranes using novel TEM techniques. *Journal of Membrane Science*, *358*(1), 51-59. https://doi.org/10.1016/j.memsci.2010.04.032

Rames, M., Yu, Y., & Ren, G. (2014). Optimized negative staining : A high-throughput protocol for examining small and asymmetric protein structure by electron

microscopy. *Journal of Visualized Experiments : JoVE, 90*, e51087. https://doi.org/10.3791/51087

Ripper, D., Schwarz, H., & Stierhof, Y.-D. (2008). Cryo-section immunolabelling of difficult to preserve specimens : Advantages of cryofixation, freeze-substitution and rehydration. *Biology of the Cell*, *100*(2), 109-123. https://doi.org/10.1042/BC20070106

Roberge, H., Moreau, P., Couallier, E., & Abellan, P. (2022). Determination of the key structural factors affecting permeability and selectivity of PAN and PES polymeric filtration membranes using 3D FIB/SEM. *Journal of Membrane Science*, *653*, 120530. https://doi.org/10.1016/j.memsci.2022.120530

Rouquié, C., Liu, S., Rabiller-Baudry, M., Riaublanc, A., Frappart, M., Couallier, E., & Szymczyk, A. (2020). Electrokinetic leakage as a tool to probe internal fouling in MF and UF membranes. *Journal of Membrane Science*, *599*, 117707. https://doi.org/10.1016/j.memsci.2019.117707

Rouquié, C., Szymczyk, A., Rabiller-Baudry, M., Roberge, H., Abellan, P., Riaublanc, A., Frappart, M., Álvarez-Blanco, S., & Couallier, E. (2022). NaCl precleaning of microfiltration membranes fouled with oil-in-water emulsions : Impact on fouling dislodgment. *Separation and Purification Technology*, *285*, 120353.

Rudolph, G., Virtanen, T., Ferrando, M., Güell, C., Lipnizki, F., & Kallioinen, M. (2019). A review of in situ real-time monitoring techniques for membrane fouling in the biotechnology, biorefinery and food sectors. *Journal of Membrane Science*, *588*, 117221. https://doi.org/10.1016/j.memsci.2019.117221

Ruste, J. (1987). *Chapter XI EDS and WDS spectrometry : Processing of spectrum*. 32.

Safi, C., Olivieri, G., Campos, R. P., Engelen-Smit, N., Mulder, W. J., van den Broek, L. A. M., & Sijtsma, L. (2017). Biorefinery of microalgal soluble proteins by sequential

processing and membrane filtration. In *Bioresour Technol* (Vol. 225, p. 151-158). https://doi.org/10.1016/j.biortech.2016.11.068

Sarraf, C. E. (2000). Immunolabeling for electron microscopy. *Methods in Molecular Medicine*, *40*, 439-452. https://doi.org/10.1385/1-59259-076-4:439

Sato, C., Yamazawa, T., Ohtani, A., Maruyama, Y., Memtily, N., Sato, M., Hatano, Y., Shiga, T., & Ebihara, T. (2019). Primary cultured neuronal networks and type 2 diabetes model mouse fatty liver tissues in aqueous liquid observed by atmospheric SEM (ASEM) : Staining preferences of metal solutions. *Micron*, *118*, 9-21. https://doi.org/10.1016/j.micron.2018.11.005

Stradner, A., Sedgwick, H., Cardinaux, F., Poon, W. C. K., Egelhaaf, S. U., & Schurtenberger, P. (2004). Equilibrium cluster formation in concentrated protein solutions and colloids. *Nature*, *432*(7016), Article 7016. https://doi.org/10.1038/nature03109

Sundaramoorthi, G., Hadwiger, M., Ben-Romdhane, M., Behzad, A. R., Madhavan, P., & Nunes, S. P. (2016). 3D Membrane Imaging and Porosity Visualization. *Industrial & Engineering Chemistry Research*, *55*(12), Article 12. https://doi.org/10.1021/acs.iecr.6b00387

Suwal, S., Doyen, A., & Bazinet, L. (2015). Characterization of protein, peptide and amino acid fouling on ion-exchange and filtration membranes : Review of current and recently developed methods. *Journal of Membrane Science*, *496*, 267-283. https://doi.org/10.1016/j.memsci.2015.08.056

Thompson, R. F., Walker, M., Siebert, C. A., Muench, S. P., & Ranson, N. A. (2016). An introduction to sample preparation and imaging by cryo-electron microscopy for structural biology. *Methods*, *100*, 3-15. https://doi.org/10.1016/j.ymeth.2016.02.017

Trent, J. S. (1984). Ruthenium tetraoxide staining of polymers : New preparative methods for electron microscopy. *Macromolecules*, *17*(12), Article 12. https://doi.org/10.1021/ma00142a087

Trent, J. S., Scheinbeim, J. I., & Couchman, P. R. (1983). Ruthenium tetraoxide staining of polymers for electron microscopy. *Macromolecules*, *16*(4), 589-598. https://doi.org/10.1021/ma00238a021

Tummons, E., Han, Q., Tanudjaja, H. J., Hejase, C. A., Chew, J. W., & Tarabara, V. V. (2020). Membrane fouling by emulsified oil : A review. *Separation and Purification Technology*, *248*, 116919. https://doi.org/10.1016/j.seppur.2020.116919

Ursu, A.-V., Marcati, A., Sayd, T., Sante-Lhoutellier, V., Djelveh, G., & Michaud, P. (2014). Extraction, fractionation and functional properties of proteins from the microalgae Chlorella vulgaris. In *Bioresource Technology* (Vol. 157, Numéro 0, p. 134-139). http://dx.doi.org/10.1016/j.biortech.2014.01.071

Villafaña-López, L., Clavijo Rivera, E., Liu, S., Couallier, E., & Frappart, M. (2019). Shear-enhanced membrane filtration of model and real microalgae extracts for lipids recovery in biorefinery context. *Bioresource Technology*, *288*, 121539. https://doi.org/10.1016/j.biortech.2019.121539

Yu, Z., Chu, H., Zhang, W., Gao, K., Yang, L., Zhang, Y., & Zhou, X. (2021). Multi-dimensional in-depth dissection the algae-related membrane fouling in heterotrophic microalgae harvesting : Deposition dynamics, algae cake formation, and interaction force analysis. *Journal of Membrane Science*, *635*, 119501. https://doi.org/10.1016/j.memsci.2021.119501